



# Past abrupt changes, tipping points and cascading impacts in the Earth system

Victor Brovkin <sup>1,2</sup>✉, Edward Brook<sup>3</sup>, John W. Williams <sup>4</sup>, Sebastian Bathiany<sup>5</sup>, Timothy M. Lenton <sup>6</sup>, Michael Barton<sup>7</sup>, Robert M. DeConto <sup>8</sup>, Jonathan F. Donges <sup>9,10</sup>, Andrey Ganopolski<sup>9</sup>, Jerry McManus<sup>11</sup>, Summer Praetorius <sup>12</sup>, Anne de Vernal<sup>13</sup>, Ayako Abe-Ouchi <sup>14</sup>, Hai Cheng <sup>15</sup>, Martin Claussen <sup>1,16</sup>, Michel Crucifix<sup>17</sup>, Gilberto Gallopín<sup>18</sup>, Virginia Iglesias <sup>19</sup>, Darrell S. Kaufman<sup>20</sup>, Thomas Kleinen <sup>1</sup>, Fabrice Lambert <sup>21</sup>, Sander van der Leeuw<sup>22</sup>, Hannah Liddy <sup>23</sup>, Marie-France Loutre <sup>24</sup>, David McGee <sup>25</sup>, Kira Rehfeld <sup>26</sup>, Rachael Rhodes <sup>27</sup>, Alistair W. R. Seddon<sup>28</sup>, Martin H. Trauth <sup>29</sup>, Lilian Vanderveken<sup>17</sup> and Zicheng Yu <sup>30,31</sup>

**The geological record shows that abrupt changes in the Earth system can occur on timescales short enough to challenge the capacity of human societies to adapt to environmental pressures. In many cases, abrupt changes arise from slow changes in one component of the Earth system that eventually pass a critical threshold, or tipping point, after which impacts cascade through coupled climate–ecological–social systems. The chance of detecting abrupt changes and tipping points increases with the length of observations. The geological record provides the only long-term information we have on the conditions and processes that can drive physical, ecological and social systems into new states or organizational structures that may be irreversible within human time frames. Here, we use well-documented abrupt changes of the past 30 kyr to illustrate how their impacts cascade through the Earth system. We review useful indicators of upcoming abrupt changes, or early warning signals, and provide a perspective on the contributions of palaeoclimate science to the understanding of abrupt changes in the Earth system.**

There is increasing awareness and concern that human modification of the environment runs the risk of inducing abrupt changes in a variety of Earth system components<sup>1</sup> (Box 1). Disintegration of ice sheets, permafrost thaw, slowdown of ocean circulation, tropical and boreal forest dieback and ocean deoxygenation are examples of rapid changes with harmful societal consequences that might happen in the future due to ongoing anthropogenic climate change. Analogous events have occurred in the recent geological past<sup>2</sup> (Fig. 1). To use them for understanding possible consequences of future climate change, we must quantify the characteristics and timing of the initial abrupt change during these past events, the tipping points involved and the subsequent sequence of cascading consequences for other components (Box 1).

Here, we follow the Intergovernmental Panel on Climate Change Assessment Report 4 (IPCC AR4)<sup>3</sup> definition of abrupt changes (events) as large-scale changes that are much faster than the change in the relevant forcing, such as rising atmospheric CO<sub>2</sub> concentrations (Box 1). In addition, we assess evidence for past tipping points, or thresholds, beyond which components of the Earth system rapidly move to a new state, but take much longer to return to the original state even when forcings abate (Box 1). Forcings evolve frequently in the Earth system, but do not always reach the tipping points that might lead to abrupt changes. For instance, regional droughts interspersed with occasional wet periods may not generally have a strong effect on ecosystems adapted to such a climate state. However, if a drought persists over many years (megadroughts<sup>4</sup>),

<sup>1</sup>Max Planck Institute for Meteorology, Hamburg, Germany. <sup>2</sup>CEN, Universität Hamburg, Hamburg, Germany. <sup>3</sup>College of Earth, Ocean, and Atmospheric Sciences, Oregon State University, Corvallis, OR, USA. <sup>4</sup>Department of Geography and Center for Climatic Research, University of Wisconsin-Madison, Madison, WI, USA. <sup>5</sup>Climate Service Center Germany (GERICS), Helmholtz-Zentrum Hereon, Hamburg, Germany. <sup>6</sup>Global Systems Institute, University of Exeter, Exeter, UK. <sup>7</sup>School of Human Evolution and Social Change and School of Complex Adaptive Systems, Arizona State University, Tempe, AZ, USA. <sup>8</sup>Department of Geosciences, University of Massachusetts, Amherst, MA, USA. <sup>9</sup>Earth System Analysis, Potsdam Institute for Climate Impact Research, Potsdam, Germany. <sup>10</sup>Stockholm Resilience Centre, Stockholm University, Stockholm, Sweden. <sup>11</sup>Lamont-Doherty Earth Observatory, Columbia University, Palisades, NY, USA. <sup>12</sup>Geology, Minerals, Energy and Geophysics Science Center, US Geological Survey, Menlo Park, CA, USA. <sup>13</sup>Geotop Research Center, Université du Québec à Montréal, Montreal, Canada. <sup>14</sup>Atmosphere and Ocean Research Institute, The University of Tokyo, Tokyo, Japan. <sup>15</sup>Institute of Global Environmental Change, Xi'an Jiaotong University, Shaanxi, China. <sup>16</sup>Institute for Meteorology, Universität Hamburg, Hamburg, Germany. <sup>17</sup>Earth and Life Institute, UCLouvain, Louvain-la-Neuve, Belgium. <sup>18</sup>Independent Researcher, Buenos Aires, Argentina. <sup>19</sup>Earth Lab, University of Colorado, Boulder, CO, USA. <sup>20</sup>School of Earth and Sustainability, Northern Arizona University, Flagstaff, AZ, USA. <sup>21</sup>Institute of Geography, Pontifical Catholic University of Chile, Santiago de Chile, Chile. <sup>22</sup>School of Sustainability, Arizona State University, Tempe, AZ, USA. <sup>23</sup>Center for Climate Systems Research, Columbia University, New York, NY, USA. <sup>24</sup>PAGES (Past Global Changes), Bern, Switzerland. <sup>25</sup>Earth, Atmospheric and Planetary Sciences, Massachusetts Institute of Technology, Cambridge, MA, USA. <sup>26</sup>Institute of Environmental Physics, Ruprecht-Karls Universität Heidelberg, Heidelberg, Germany. <sup>27</sup>Department of Earth Sciences, University of Cambridge, Cambridge, UK. <sup>28</sup>Department of Biology and Bjerknes Centre for Climate Research, University of Bergen, Bergen, Norway. <sup>29</sup>Institute of Geosciences, University of Potsdam, Potsdam, Germany. <sup>30</sup>Department of Earth and Environmental Sciences, Lehigh University, Bethlehem, PA, USA. <sup>31</sup>Institute for Peat and Mire Research, School of Geographical Sciences, Northeast Normal University, Changchun, China.

✉e-mail: [victor.brovkin@mpimet.mpg.de](mailto:victor.brovkin@mpimet.mpg.de)

**Box 1 | Terminology**

**Abrupt change** refers to large-scale change that is much faster than the change in the relevant forcing<sup>3</sup>. Both the amplitude (scale) and relative rates of forcing and response changes are important. In the palaeo context, the relevant forcing is usually the Earth orbital forcing with a multimillennial timescale (the fastest component of the orbital forcing, the precessional cycle, has a periodicity of 19 kyr).

**Cascading impacts** are a sequence of events where abrupt changes in one component lead to abrupt changes in other components. These changes could also interact with each other and propagate from larger to smaller spatial scales or vice versa (Fig. 2).

**Early Warning Signals (EWS)** are quantitative indicators of the proximity of a system to a tipping point<sup>74</sup>. EWS apply mathematical principles of dynamical systems to Earth system components. EWS could be measured in one-dimensional space (such as time series of dust deposition in a marine core) using univariate precursors (for example, increasing temporal autocorrelation) or in multi-dimensional space (such as spatial patterns of vegetation cover) applying spatially explicit precursors (Table 2).

**Earth system components** are the atmosphere, ocean, cryosphere, biosphere and anthroposphere. These can be further divided into subcomponents such as monsoon systems, ocean circulation, sea ice, different ecosystems and human (social) systems.

**Forcing** refers to a factor that influences the system dynamics. For example, Earth system forcings include incoming solar radiation,

concentrations of greenhouse gases in the atmosphere and volcanic eruptions. For Earth system components and subcomponents, forcings could be changes in the other components leading to cascading impacts.

**Irreversible change** denotes a change that is irreversible if the recovery timescale to the state before change is substantially longer than the time it takes for the system to reach this state<sup>3</sup>.

**State** refers to a set of variables that describes the state of a dynamical system. These could be climate variables (air temperature, stream velocity in the ocean), ecological variables (number of species, plant biomass) or societal variables (population density, income).

**Tipping points** are critical thresholds (in forcings or in a system) at which a small perturbation can nonlinearly alter the state or development of a system<sup>1</sup>. Tipping points combine different types of phenomenon inasmuch as thresholds could be explicit (for example, 0°C for ice) or hidden (such as small reduction in insolation leading to a snowball Earth). The latter can indicate a co-existence of two stable states (for example, snowball and ice-free), with one state becoming unstable.

**Autocorrelation** is the correlation between an observational time series and its copy shifted by a certain time lag. **Skewness** is a measure of the asymmetry of the data distribution. A **univariate precursor** is a function of one variable. **Variance** is a measure of how far a dataset is spread out from its average.

the water available for plants could drop below a critical threshold, leading to a cascade of abrupt changes in vegetation cover, agriculture and societies that may be irreversible in the coming decades to centuries<sup>5,6</sup>.

A rapidly growing archive of palaeoclimatic, palaeoecological and archaeological records is particularly useful for understanding the ways in which abrupt change emerges from the interaction among system components and can cascade across components and scales. Here, we consider cascading interactions where abrupt changes in one component have led to abrupt changes in other components<sup>7</sup> (Box 1). Causality in such cascading interactions can be difficult to prove from palaeo records alone, and the predictive power of past causalities for future events is limited by different timescales and forcings. However, we can infer causal interactions if there is sufficient evidence and consistency in the relative timing of changes, understanding of processes and, if available, support from Earth system model experiments.

Gleaning useful information from palaeo archives requires putting this evidence into consistent temporal, spatial and conceptual frameworks. It is especially hard to infer causality in interactions among Earth system components. Existing work on these interactions suggests that the majority of cascading changes proceed from larger to smaller spatial scales<sup>8</sup>. Hence, we structure this Review to consider causality generally flowing from climate to ecological and sometimes to social systems, focusing on the cascading of abrupt changes from one component to another, with particular attention to cryosphere–ocean interactions and hydroclimate variability (Fig. 2). These two important classes of abrupt changes are the most prominent examples with the requisite number or quality of palaeo records, and probably have important societal impacts in the near future.

**Cascading impacts of cryosphere–ocean interactions**

Interactions between the cryosphere and oceans have produced some of the most dramatic events in the geological record, including

glacial outburst floods and repeated catastrophic iceberg discharges during past glaciations (Table 1). Model simulations of the ocean–atmosphere dynamics consistently show that the vertical convection in the North Atlantic, as well as the advective fluxes associated with the Atlantic Meridional Overturning Circulation (AMOC), may be weakened or even stopped (shut down) by pulses of freshwater into the surface ocean at high northern latitudes<sup>9</sup>. These circulation changes are associated with a specific spatial pattern, often referred to as a bipolar seasaw<sup>10</sup>, including a southward shift of the Intertropical Convergence Zone, substantial cooling in the Northern Hemisphere centred in the North Atlantic region and general warming in the Southern Hemisphere. Palaeoclimate data from ice cores reveal the persistence of such a bipolar pattern of climate on millennial timescales during the last ice age and the deglaciation (around 19–12 kyr ago (ka))<sup>10</sup>, and evidence from deep-sea sediments confirms that these abrupt climate changes were associated with substantial changes in the AMOC<sup>11,12</sup>. The cause of these changes in the AMOC is widely believed to be related to cryosphere–ocean interactions. The likely candidate mechanisms, including surging ice sheets<sup>13</sup>, ice-shelf breakup<sup>14</sup>, a coupled ocean–ice ‘salt oscillator’<sup>15</sup>, catastrophic ice stream retreat<sup>16</sup> and deep ocean warming due to deglaciation<sup>17</sup>, are all considered to be threshold responses to slowly varying forcing (Fig. 2a).

About twenty climate fluctuations known as Dansgaard–Oeschger (D–O) events occurred during the last glacial cycle. The abrupt onsets of warming in these events on decadal timescales<sup>18</sup> correspond to temperature increases that may have exceeded 15°C in Greenland and several degrees Celsius in Europe, and are generally followed by a multi-century cooling trend and terminated by an abrupt return to the glacial baseline<sup>19</sup>. These events caused major adjustments to hydroclimate and carbon cycling<sup>20–22</sup>, with evidence for crossing of regional thresholds in marine ecosystems (such as a change to anoxic deep water conditions in the Cariaco Basin<sup>23</sup>) and terrestrial ecosystems (for example, forest expansion in western Mediterranean region<sup>24</sup>, the extirpation of Holarctic megafaunal

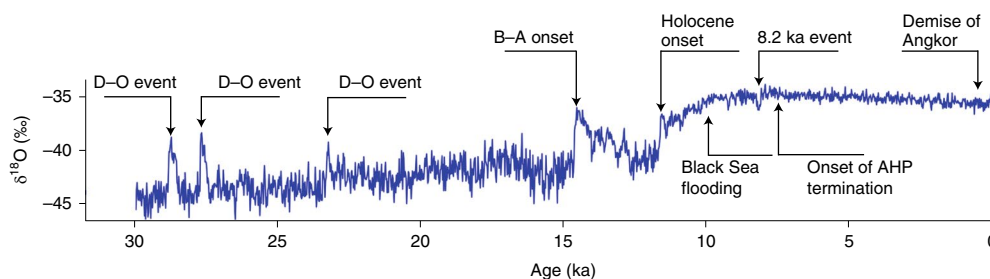


**Fig. 1 | Timeline of abrupt events over the past 30 kyr overlaid on a  $\delta^{18}\text{O}$  time series.** The  $\delta^{18}\text{O}$  time series is from North Greenland Ice Core Project<sup>44</sup>. AHP, African Humid Period; D-O, Dansgaard-Oeschger event; B-A, Bølling-Allerød warm period.

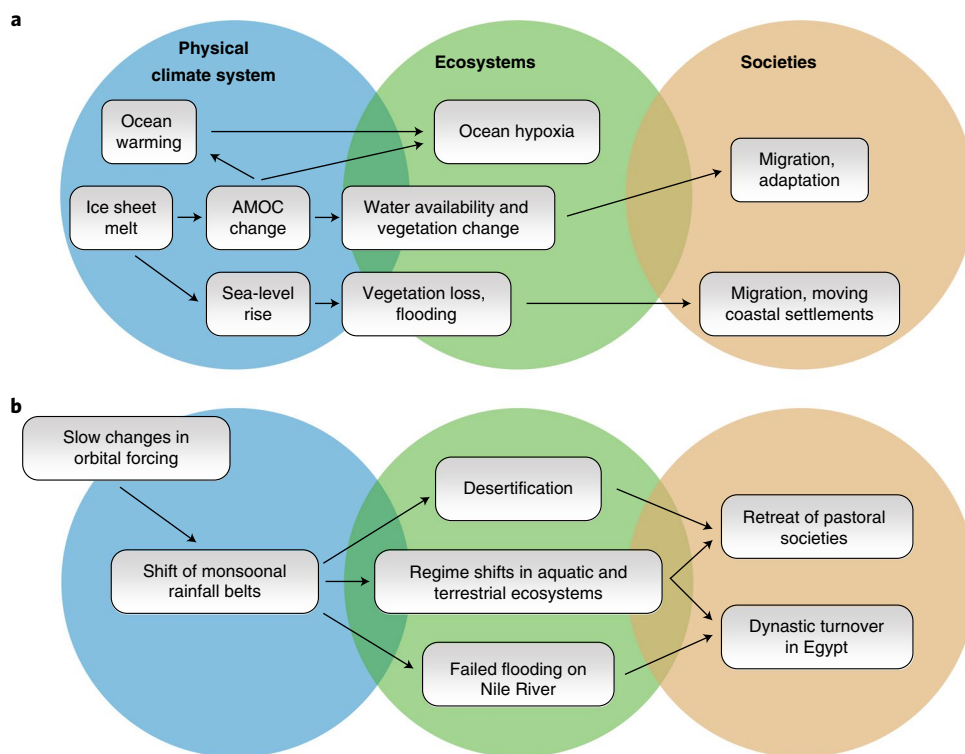


**Fig. 2 | Cascades of abrupt changes in physical-ecological-societal components of the Earth system.** **a**, Onset of the Bølling-Allerød warm period. **b**, Termination of the AHP.

species<sup>25</sup> (Table 1) and abrupt increases in methane emissions from wetlands<sup>26</sup>) (Fig. 3). The D-O events demonstrate that global-scale reorganization of the climate system can occur on decadal timescales<sup>27</sup>, possibly triggered by abrupt changes in the AMOC. Although the focus is often on meltwater as the driver of AMOC reduction and Northern Hemisphere cooling, the onset of D-O warming is extremely abrupt and typically exceeds the rate of cooling into stadial events. These rapid fluctuations suggest that AMOC recovery can occur on even faster timescales than a shutdown<sup>18,28</sup>.

During the rapid deglacial transition into the Bølling-Allerød warm period (14.7–12.9 ka), abrupt changes cascaded through the whole Earth system (Figs. 1, 2a and 3). The strengthening of the AMOC<sup>12</sup>, rapid sea-level rise during the Meltwater Pulse 1 event<sup>29</sup> and an abrupt increase in atmospheric  $\text{CO}_2$  and  $\text{CH}_4$  concentrations<sup>26</sup> (Fig. 3) led to abrupt changes in the terrestrial climate, water availability<sup>30</sup> and vegetation composition in the Northern<sup>31–33</sup> and Southern<sup>34</sup> hemispheres (Table 1 and Supplementary Information). In addition, marine records from low-oxygen regions document rapid shifts to sedimentary hypoxia (Fig. 3 and Supplementary

Information). These records include evidence for an expansion of the oxygen minimum zone across the North Pacific<sup>35</sup>, as well as shifts to more severe hypoxia in the Cariaco Basin<sup>23</sup> and Arabian Sea<sup>36</sup>, suggesting a persistent link between warming and ocean deoxygenation that transcends regional patterns of circulation and productivity. In the North Pacific, the abrupt onset of hypoxia occurred in conjunction with rapid warming of surface waters by 4–5 °C (ref. <sup>37</sup>). Rates of onset of severe hypoxia were on century timescales or possibly faster<sup>38</sup> (Fig. 3 and Supplementary Information), while benthic faunal recovery lasted 1–2 kyr, representing recovery time periods that were at least ten times longer than the onsets<sup>37</sup>.

Past sea-level rises linked to ice sheet collapses have sometimes caused abrupt flooding events with ecological and social consequences. The best-quantified rates during these rapid rises exceed 20 m kyr<sup>-1</sup> (ref. <sup>39</sup>) (Figs. 2a and 3 and Supplementary Information). The flooding was more abrupt at local to regional scales. A particularly prominent example of abrupt flooding is the Black Sea (Table 1), which has a sill depth across the Strait of Bosphorus that today is 35 m below sea level. As ice sheets melted, and sea level

**Table 1 | Examples of abrupt events and tipping points in the past 30 kyr**

Abrupt event/ tipping point	Date(s)	Rapidity of event	Effects in Earth system components	
			Climate, cryosphere and hydrosphere	Land and marine ecosystems; atmospheric CO <sub>2</sub> and CH <sub>4</sub> ; societies
Onset of D–O events	28.9, 27.7 and 23.3 ka (refs. 18,44)	<30 yr (ref. 19)	8–16 °C of warming in Greenland <sup>19</sup> ; intensification of the Asian summer monsoon <sup>51</sup> ; weakening of the South American summer monsoon <sup>21</sup>	Afforestation from grasslands to wooded steppes in Europe <sup>31</sup> ; Holarctic megafauna extirpations <sup>25</sup> ; expanded oxygen minimum zones (for example, Cariaco Basin) <sup>23</sup> ; abrupt increase in atmospheric CH <sub>4</sub> (ref. 22)
Onset of Bølling–Allerød warming	14.7 ka (ref. 19)	1–3 yr (refs. 18,44)	9–14 °C of warming in Greenland <sup>19</sup> ; 4–5 °C of sea surface temperature warming in the North Pacific <sup>37</sup> ; rapid ice sheet melt, acceleration of sea-level rise (meltwater pulse) <sup>29,39</sup> ; drying in southwestern North America <sup>30</sup> ; intensification of the West African <sup>53</sup> and Asian summer monsoons <sup>51</sup> ; weakening of the South American summer monsoon <sup>34</sup>	Rapid afforestation of tundra (Scandinavia), expansion of species from glacial refugia <sup>32</sup> ; expansion of oxygen minimum zones and contraction of marine benthic diversity (North Pacific) <sup>35,37</sup> ; abrupt increase in atmospheric CH <sub>4</sub> and CO <sub>2</sub> <sup>26</sup>
Onset of the Holocene	11.7 ka (ref. 44)	<60 yr (refs. 18,44)	8–12 °C of warming in Greenland <sup>19</sup> , 4–6 °C of warming in western Europe; 4–5 °C increase in sea surface temperature in the northeast Pacific and North Atlantic; monsoon impacts similar to Bølling–Allerød warming <sup>51</sup>	Similar to the impacts of Bølling–Allerød warming (except atmospheric CO <sub>2</sub> ) <sup>32</sup>
Black Sea flooding	9.5–9.0 ka (ref. 41)	<40 yr (ref. 41)	Rapid flooding of surrounding shelves and subsequent salinification of the Black Sea basin, sea level rise of >10 m <sup>41</sup>	Drowning of land ecosystems and settlements on the shelf, coastal erosion, a shift from freshwater to saltwater ecosystems and anoxia in the deep basin <sup>41</sup>
8.2 ka event	8.2 ka (ref. 44)	5 yr (refs. 18,44)	3–4 °C of cooling in Greenland <sup>48</sup>	Rapid plant community turnover, declines of thermophilous species <sup>49</sup>
Holocene aridification; end of the AHP	8–3 ka, timing varies regionally	100–1,000 yr (ref. 53)	Waning of monsoon rainfall in North Africa <sup>53,60</sup> ; drying in southwestern and midcontinental North America <sup>65</sup>	Regionally rapid southward shift of North African grasslands <sup>53,59,64</sup> ; an eastward shift of prairie–forest ecotones, activation of dunes, C <sub>3</sub> /C <sub>4</sub> plant shifts and altered fire regimes in central North America <sup>69</sup>
Holocene megadroughts	High variability 5.4–4 ka; past 2 ka (ref. 47)	1–10 yr	Water shortage, extreme drought, decrease of groundwater levels <sup>47</sup>	Slowed tree growth rates, mortality of mesic tree species and abandonment of early agricultural sites <sup>6,47,67</sup>

gradually rose to the level of the Black Sea sill at approximately 9.5–9.0 ka, seawater spilled into the basin, raising sea level in the Black Sea by more than 10 m within a few decades<sup>40,41</sup>. This flooding established a connection to the sea that includes saltwater inflow at depth and fresher outflow at the surface<sup>41</sup>, creating an anoxic and sulfate-reducing deep basin. Other examples of deglacial sea-level flooding include Doggerland between the modern British Isles and mainland Europe, where the Channel River or Fleuve Manche palaeo-river gave way to the repeated deglacial inundations that most recently resulted in the modern English Channel and North Sea<sup>42</sup>, and the broad Sunda Shelf with abrupt submergence period between 14.6 and 14.3 ka (ref. 43). In each of these cases, crossing regional-scale thresholds in response to a gradual rise of sea level resulted in new and dramatically different states that, in places, presumably altered the trajectories of early human societies.

### Cascading impacts of hydroclimate variability

Hydroclimate variability (changes in land climate and hydrology) in the current interglacial, the Holocene (started 11.7 ka; ref. 44), represents the most vivid example of cascading abrupt changes relevant to the present day. The Holocene is often considered a period of relatively stable climate and a ‘safe operating space’ for humankind<sup>45</sup>. While this is true globally, geological records show a number of abrupt changes originating and cascading through coupled climate, ecological and social systems on regional scales<sup>46,47</sup>. For example,

an abrupt climate event at about 8.2 ka, caused by ice-sheet meltwater discharge into the North Atlantic, led to cold and dry conditions in the Northern Hemisphere<sup>48</sup> visible in rapid changes in vegetation composition in Europe<sup>49</sup> and North America (Table 1 and Supplementary Information). Key characteristics of the current interglacial include a warm and hydrologically variable atmosphere, a growing anthropogenic footprint<sup>50</sup> and multiple instances of abrupt change in hydroclimate<sup>51</sup>, vegetation<sup>52</sup> and societies<sup>46</sup>.

Hydroclimate variability during the Holocene was partially forced by slow variations in Earth’s orbit on millennial timescales<sup>53</sup> and solar activity on centennial timescales<sup>54</sup>. Decadal-scale clusters of volcanic eruptions were probably responsible for abrupt cooling in the sixth century that led to famine and societal reorganization in Europe (transformation of the eastern Roman Empire) and Asia (a rise of the Arabic Empire)<sup>55</sup>. Many of the most severe megadroughts (decadal-scale droughts) seem to represent unforced variability in the ocean–atmosphere system, such as the El Niño/Southern Oscillation<sup>4</sup>. Megadroughts during the Holocene were larger and more intense than any observed in twentieth- and twenty-first-century instrumental records. In North America, multiple episodes of droughts and abrupt ecosystem changes are identified from 10.7 to 0.6 ka (ref. 47), with the earliest abrupt moisture decrease at 9.4 ka probably linked to meltwater pulses into the North Atlantic. Widespread megadroughts and synchronous societal collapse and reorganization have been reported at

**Table 2 | Precursors of past abrupt changes in climate–ecological–societal systems**

Abrupt changes	Source and methods of detection	Univariate precursors	Spatially explicit precursors
AMOC collapse	Modelled and reconstructed changes <sup>9–12</sup>	Observations too short and reconstructions too uncertain for meaningful analysis; models of different complexity suggest the existence of precursors <sup>77,78</sup>	Autocorrelation of critical spatial pattern increases in a model <sup>77</sup> ; increased autocorrelation and variance with latitude-dependent signal-to-noise ratio <sup>78</sup>
D–O events	Greenland isotope record <sup>44</sup>	Shifts argued to be noise-induced <sup>79</sup> ; increase in autocorrelation and variance in the ensemble of events, but not individual events <sup>80</sup> ; increase in autocorrelation and variance on decadal timescales preceding events <sup>18</sup>	No literature
Onset of the Holocene	Greyscale sediment record from the Cariaco Basin <sup>74</sup>	Increased autocorrelation with signal at the edge of significance <sup>74</sup>	Synchronization of North Pacific and North Atlantic climates during recent deglaciation and Younger Dryas <sup>87</sup>
End of the AHP	Dust deposition record <sup>53</sup> ; conceptual models	Inconclusive signals <sup>50,74</sup>	Pattern formation in several stages before complete desertification is observed <sup>89</sup> ; increasing spatial variance and skewness in simple models <sup>88</sup>
Monsoon changes	Reconstruction of rainfall during the Pleistocene from Chinese caves <sup>81</sup>	No consistent signals before abrupt changes in the east Asian summer monsoon <sup>81</sup>	No literature
Changes in aquatic and marine ecosystems	Reconstructions <sup>35</sup> , contemporary observations	Increasing variance in fish populations after fishing <sup>93</sup> , critical slowing down before extinctions of planktonic crustaceans <sup>95</sup>	Observed indications of increasing spatial variance before changes in shelf ecosystems <sup>83</sup>
Societal collapses and transformations	Reconstructions of past societal changes <sup>72</sup>	Increasing variance and autocorrelation before human population collapse during the European Neolithic <sup>91</sup> ; increasing variance before two cases of social transformation in the pre-Hispanic US Southwest <sup>92</sup>	No literature

4.2 ka, especially in mid- and low latitudes<sup>56</sup>, which is the basis for proposed Megahalayan stage of the Holocene. However, the cause of the 4.2 ka event remains unclear and its signal is weak in some regions, such as the northern North Atlantic<sup>57</sup>.

The propagation of abrupt change from the hydroclimate to collapses in ecological and social systems well-documented in regions around the world<sup>16,58</sup> is especially pronounced at the end of the AHP, which lasted from 15 ka to 5 ka (ref. 53) (Fig. 2b). The southward retreat of monsoonal rainfall belts in North Africa—driven by changes in the summer insolation mainly related to the climatic precession of the Earth's orbit—was frequently marked by abrupt, local-scale declines in rainfall that progressed spatially from north to south<sup>59,60</sup>. The termination of the AHP at around 5 ka occurred on a centennial, rather than decadal, timescale, but at least an order of magnitude faster than the orbital forcing changes (Supplementary Information). The termination was amplified by vegetation feedbacks, the desiccation of lakes, soil erosion and dust emissions<sup>61</sup> (Fig. 2b). Some local aquatic and terrestrial ecosystems experienced a series of abrupt changes, as thresholds were passed for individual species and ecosystems<sup>62</sup>. North African drying and vegetation changes led to a cascade of other abrupt changes. These include the collapse of complex networks of terrestrial vertebrate herbivores and carnivores, as their resource base of primary productivity was undercut<sup>63</sup>. It also includes the retreat of pastoral societies from North Africa<sup>64</sup>, the episodes of failed flooding on the Nile River and dynastic turnover from the Old to New Kingdom in Egypt<sup>58</sup>.

During the early Holocene, the Great Plains in North America were also marked by widespread regional drying on millennial timescales<sup>65</sup>, producing abrupt biome-scale changes as individual species and ecosystems passed thresholds<sup>66</sup>. Examples include the rapid replacement of C<sub>3</sub> forest and grasslands with C<sub>4</sub> grasslands<sup>67</sup>,

forest loss and eastward shifts of the prairie–forest ecotone<sup>68</sup> (Fig. 3 and Supplementary Information), altered fire regime<sup>69</sup> and lowered groundwater tables in the northern Great Plains<sup>47</sup>. In the mesic forests of eastern North America and Europe, trees such as oak and hemlock experienced major decline in abundance that have been linked to droughts and climate variability in the North Atlantic<sup>70</sup>. In southwestern North America, farming settlements experienced repeated cycles of growth in the number and size, followed by abandonment and population dispersal. These cycles were intimately linked to the expansion and contraction of maize production, which were tied to drought events whose impacts were amplified during periods of maximal growth by higher populations and more complex societal organizations<sup>71</sup>.

Hydroclimate variability, such as megadrought, is often associated with destabilization of past agricultural societies. However, it should be viewed more as a trigger of societal collapse than the sole cause. Even where the subsistence economies depended on sophisticated water management systems that required extensive cooperation and organizational management, societal resilience and collapse also involve complex interactions between multiple natural and social factors<sup>58</sup>. For example, periods of regional droughts during the past millennium<sup>6</sup> are linked with the collapses of the Khmer Empire at Angkor between ~1300 and 1500 AD (ref. 46) (Fig. 3 and Supplementary Information), the prehistorical Hohokam society in central Arizona<sup>72</sup> in the fifteenth century and the Ming Dynasty in China approximately 1600 AD (ref. 6). All three of these example societies had weathered previous hydroclimatic changes. The environmental tipping points that triggered societal breakdowns occurred in the context of pre-existing vulnerabilities created by societal dynamics: an overextended human-built hydrology system in the Khmer capital of Angkor, an increasingly hierarchical social order coupled with immigration from elsewhere in the American

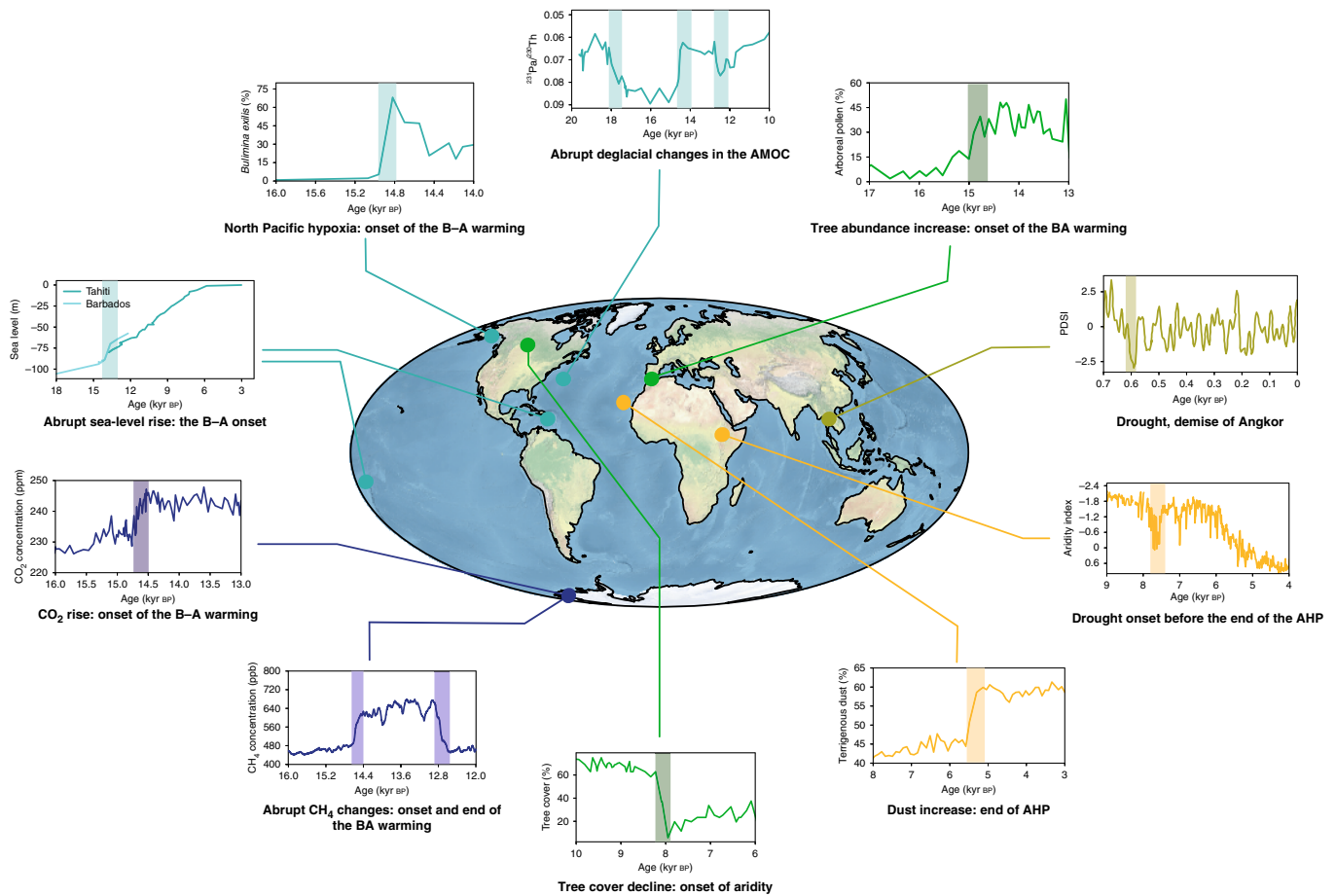


**Fig. 3 | A map of selected atmospheric, oceanographic, ecosystem and societal records with abrupt changes or tipping points in the past 20 kyr.** Dots are approximate record locations. Clockwise around the globe, the colours indicate the Earth system components: turquoise marks the ocean domain (sea-level change at Barbados<sup>39</sup> and Tahiti<sup>29</sup>; hypoxia in the North Pacific<sup>37</sup> reflected in the relative abundance of low-oxygen benthic foraminifera *Bulimina exilis*; sedimentary Pa/Th in the deep western North Atlantic indicates the strength of AMOC<sup>12</sup>); light green is the societal domain (the Palmer drought severity index (PDSI) for the demise of the Angkor society<sup>46</sup>); yellow marks environment-societal interfaces (drought index for the onset of the AHP end, marked by 14 short droughts including the most dramatic event from 7.9 to 7.7 kyr BP<sup>60</sup>, and the dust fraction of deep-sea sediments showing a rise in Saharan dust at end of the AHP<sup>53</sup>); bright green represents ecosystems (tree abundance increase in Western Europe during the onset of Bølling-Allerød warming<sup>24,33</sup>, expressed as percentage of arboreal to total pollen grains; decline in tree cover estimated as percent of land area in the early Holocene<sup>66,69</sup>, as local instances of broader regional to subcontinental trends) and blue marks the atmospheric domain (abrupt changes in CO<sub>2</sub> and CH<sub>4</sub> concentrations in Antarctic ice during the onset and end of Bølling-Allerød warming<sup>26</sup>). Shaded bars indicate the periods of abrupt changes or tipping points. Time series of the data plotted on the figure are available as source data.

Southwest for the Hohokam and increasing political and social unrest when drought incited peasants to revolt against the Ming.

### Palaeo records as a testbed for early warning approaches

There is growing interest in anticipating abrupt changes in coupled social and ecological systems because of their impacts<sup>7</sup>. During the past 15 years, certain features of climate variability, in particular variance and autocorrelation, have become popular as EWS of abrupt changes<sup>73</sup> (Box 1). These univariate precursors of abrupt changes have been analysed in many reconstructed and modelled time series in regions that were suspected to feature tipping points (univariate precursors in Table 2). Although the term ‘early warning’ sounds confusing for events that happened in the past, the palaeo archives are useful to test predictions of certain potential abrupt changes. For example, increased autocorrelation in the North African dust record<sup>53</sup> can be seen as an indicator of the slowing down of the hydroclimate-vegetation system, approaching instability<sup>74</sup> that is relevant for future changes.

The univariate framework is mostly based on simple, one-dimensional conceptual models. Owing to the complexity of

processes in the real world, the application of EWS faces challenges because climate variability can change due to many reasons unrelated to changes in stability<sup>75,76</sup>—a caveat that affects many of the examples in Table 2. In a nutshell, EWS are expected in a system that is in steady state with its environment and whose balance of feedbacks changes in a destabilizing way; that is, where negative (dampening) feedbacks are weakened and/or positive (destabilizing) feedbacks are strengthened. However, it is often unclear whether this shift in feedbacks dominates a system’s variability. For example, the question of whether a reorganization of the AMOC is preceded by EWS, such as an increase in autocorrelation and variance<sup>77,78</sup> (Table 2), depends on the contribution of the various mechanisms discussed above. Similarly, the uncertainties in the nature of D-O events cast doubt on whether they meet the conditions to show EWS<sup>18,78,79</sup> (Table 2). Abrupt changes caused by a sudden external forcing or the crossing of a spatial threshold (such as the Black Sea sill<sup>40,41</sup>) do not carry such EWS.

Although such process complexity limits the predictability of future abrupt changes, early warning approaches can be used to make inferences about the mechanisms behind past abrupt changes

in the climate record. Previous studies have addressed univariate precursors of abrupt changes such as the rapid onset of D–O events<sup>80</sup>, the termination of the AHP<sup>60,74</sup> and shifts in east Asian monsoon activity<sup>81</sup> (Table 2). The available palaeo records are often insufficient to confirm inferred mechanisms, because the time series are too short, the time resolution too low or the dating uncertainty too large. Such data limitations may be overcome with future palaeoclimate research, but the inherent properties of many palaeo time series, such as irregularly spaced samples and imperfect proxy representation of a state variable, must be carefully considered to avoid errors in early warning detection<sup>82</sup>.

Another important difference between the real world and the framework of early warnings is spatial complexity: the Earth's surface is heterogeneous and different locations are connected via atmospheric dynamics. This fact has inspired the search for EWS with a spatial component (spatially explicit precursors in Table 2). First, changes in the univariate signals discussed above can have different detectability at different places. For example, models show that the EWS in the advective water flux of the AMOC differ between latitudes<sup>78</sup>. Second, one can explicitly analyse spatio-temporal statistics such as spatial variance<sup>83</sup> or cross-correlations<sup>84</sup> between an area that has been destabilized and another location to infer the likelihood of instability approaching the second area. Collecting records from different but climatically coupled locations may therefore reveal more about the stability of the climate system.

Model results indicate where one should look for early warnings, or how one should combine the information from several locations<sup>77,85,86</sup>. For example, past records provide evidence that increasing correlations between North Pacific and Greenland climates preceded the abrupt deglaciation at the end of the last ice age<sup>87</sup>, and case studies about the end of the AHP have shown that information from single locations at the Earth's surface is not necessarily conclusive on a regional scale, but that increasing cross-correlations among different locations can help identify the next region that loses stability<sup>84</sup>. Past records provide evidence that increasing correlations between the climates of the North Pacific and Greenland preceded the abrupt deglaciation at the end of the last ice age<sup>87</sup>. There is also evidence that terrestrial ecosystems feature spatial correlations and patterns that are indicative of their proximity to thresholds<sup>88,89</sup>.

Spatial complexity is also related to the cascading of changes. A cascade of abrupt changes can have several manifestations: (1) a spatial propagation of an abrupt change from one location to another<sup>84</sup>; (2) the propagation from small to larger scales, for example, when the collapse of an ice sheet affects the AMOC and hence the climate on an almost global scale<sup>86</sup>; (3) vice versa, the propagation from large to smaller scales, for example, during the D–O events<sup>24</sup>; and (4) the propagation from one component of the Earth system to another (Fig. 2)<sup>90</sup>. As well as the climate system, ecological systems can show early warnings<sup>73</sup>, and some studies claim to have identified them before changes in human societies<sup>91,92</sup>. These examples support the view that EWS can potentially occur in any component of the Earth system, whether physical<sup>77</sup>, ecological<sup>93–95</sup> or societal<sup>91,92</sup>. This makes them highly relevant for a transdisciplinary approach to the coupled physical–ecological–social system. The dynamics of abrupt changes and EWS propagating through such coupled systems are explored in a conceptual way at present<sup>90,96</sup>, but more tools are becoming available that allow for an automated detection of abrupt changes<sup>97</sup> and their precursors<sup>98,99</sup>.

### Future work

How can the palaeo community further contribute to our understanding of abrupt changes? For palaeoclimatologists, palaeoecologists and archaeologists, the main task is twofold. First, the precision, resolution, spatial coverage and reproducibility of palaeo-environmental records must be quantitatively improved. This is necessary for identifying EWS<sup>73,95</sup>, which remains difficult due to

low-density data networks and the insufficient resolution and/or precision of the records (Table 2). The potential to test precursors of abrupt changes using palaeo records is not yet fully exploited. Second, the complex picture of feedbacks and linkages between Earth system components calls for a synthesis of data during periods of abrupt changes, including connections between natural and social systems<sup>6</sup>. The synthesis of spatial and temporal patterns of past abrupt changes is crucial to reconstructing the propagation of the signal, such as AMOC disruption, to the other domains of the Earth system<sup>87</sup>. For Earth system modellers, the main task is the further improvement of their models of coupled atmosphere–ocean–biosphere–cryosphere processes. Good progress is being made with Earth system models<sup>100</sup>; they are capable of simulating some abrupt changes, especially in the cryosphere, during the past century and in future projections<sup>101</sup>. However, they are challenged by attempts to reconstruct abrupt events that are well documented from the past, including meltwater pulses due to ice sheet collapses<sup>29</sup>, the rapid release of CO<sub>2</sub> during deglaciation<sup>26</sup> and abrupt climate and vegetation changes in North Africa during the termination of the AHP<sup>53,102</sup>. An important limitation to overcome is the ability to simulate abrupt processes on a coarse grid. Current sub-grid-scale parameterizations in Earth system models are better suited to simulating gradual, rather than abrupt, changes—as shown, for example, for permafrost thaw<sup>103</sup>. Increasing model resolution and improving sub-grid-scale parameterizations are therefore promising avenues.

Humans will always strive to anticipate the future. We are now well aware that complex systems, including the coupled social and ecological systems that now dominate our planet, can undergo abrupt changes. Constraining Earth system models to better simulate past abrupt changes is a joint task for modellers and data-gatherers. If we cannot model abrupt changes in the past, we cannot hope to predict them in the future.

### Data availability

Source data are provided with this paper.

Received: 26 July 2019; Accepted: 4 June 2021;

Published online: 29 July 2021

### References

- Lenton, T. M. et al. Tipping elements in the Earth's climate system. *Proc. Natl Acad. Sci. USA* **105**, 1786–1793 (2008).
- Lohmann, G., Butzin, M., Eissner, N., Shi, X. & Stepanek, C. Abrupt climate and weather changes across time scales. *Paleoceanogr. Paleoclimatol.* **35**, e2019PA003782 (2020).
- Meehl, G. A. & Stocker, T. F. *Global Climate Projections* (Cambridge Univ. Press, 2007).
- Steiger, N. J. et al. Oceanic and radiative forcing of medieval megadroughts in the American Southwest. *Sci. Adv.* **5**, eaax0087 (2019).
- Lustig, T., Klassen, S., Evans, D., French, R. & Moffat, I. Evidence for the breakdown of an Angkorian hydraulic system, and its historical implications for understanding the Khmer Empire. *J. Archaeol. Sci. Rep.* **17**, 195–211 (2018).
- Cook, E. R. et al. Asian monsoon failure and megadrought during the last millennium. *Science* **328**, 486–489 (2010).
- Lenton, T. M. et al. Climate tipping points—too risky to bet against. *Nature* **575**, 592–595 (2019).
- Rocha, J. C., Peterson, G., Bodin, O. & Levin, S. Cascading regime shifts within and across scales. *Science* **362**, 1379–1383 (2018).
- Ganopolski, A. & Rahmstorf, S. Rapid changes of glacial climate simulated in a coupled climate model. *Nature* **409**, 153–158 (2001).
- Pedro, J. B. et al. The last deglaciation: timing the bipolar seesaw. *Clim. Past* **7**, 671–683 (2011).
- Lynch-Stieglitz, J. The Atlantic meridional overturning circulation and abrupt climate change. *Annu. Rev. Mar. Sci.* **9**, 83–104 (2017).
- McManus, J. F., Francois, R., Gherardi, J. M., Keigwin, L. D. & Brown-Leger, S. Collapse and rapid resumption of Atlantic meridional circulation linked to deglacial climate changes. *Nature* **428**, 834–837 (2004).
- Broecker, W. S., Bond, G., Klas, M., Bonani, G. & Wolfli, W. A salt oscillator in the glacial Atlantic? 1. The concept. *Paleoceanogr. Paleoclimatol.* **5**, 469–477 (1990).

14. Gasson, E. G. W., DeConto, R. M., Pollard, D. & Clark, C. D. Numerical simulations of a kilometre-thick Arctic ice shelf consistent with ice grounding observations. *Nat. Commun.* **9**, 1510 (2018).
15. MacAyeal, D. R. Binge/purge oscillations of the Laurentide ice sheet as a cause of the North Atlantic's Heinrich Events. *Paleoceanography* **8**, 775–784 (1993).
16. Bassis, J. N., Petersen, S. V. & Mac Cathles, L. Heinrich events triggered by ocean forcing and modulated by isostatic adjustment. *Nature* **542**, 332–334 (2017).
17. Obase, T. & Abe-Ouchi, A. Abrupt Bölling-Allerød warming simulated under gradual forcing of the last deglaciation. *Geophys. Res. Lett.* **46**, 11397–11405 (2019).
18. Boers, N. Early-warning signals for Dansgaard-Oeschger events in a high-resolution ice core record. *Nat. Commun.* **9**, 2556 (2018).
19. Wolff, E. W., Chappellaz, J., Blunier, T., Rasmussen, S. O. & Svensson, A. Millennial-scale variability during the last glacial: the ice core record. *Quat. Sci. Rev.* **29**, 2828–2838 (2010).
20. Bereiter, B. et al. Mode change of millennial CO<sub>2</sub> variability during the last glacial cycle associated with a bipolar marine carbon seesaw. *Proc. Natl Acad. Sci. USA* **109**, 9755–9760 (2012).
21. Kanner, L. C., Burns, S. J., Cheng, H. & Edwards, R. L. High-latitude forcing of the South American summer monsoon during the last glacial. *Science* **335**, 570–573 (2012).
22. Bauska, T. K., Marcott, S. A. & Brook, E. J. Abrupt changes in the global carbon cycle during the last glacial period. *Nat. Geosci.* **14**, 91–96 (2021).
23. Gibson, K. A. & Peterson, L. C. A 0.6 million year record of millennial-scale climate variability in the tropics. *Geophys. Res. Lett.* **41**, 969–975 (2014).
24. Goni, M. F. S. et al. Contrasting impacts of Dansgaard-Oeschger events over a western European latitudinal transect modulated by orbital parameters. *Quat. Sci. Rev.* **27**, 1136–1151 (2008); corrigendum **27**, 1789 (2008).
25. Cooper, A. et al. Abrupt warming events drove Late Pleistocene Holarctic megafaunal turnover. *Science* **349**, 602–606 (2015).
26. Marcott, S. A. et al. Centennial-scale changes in the global carbon cycle during the last deglaciation. *Nature* **514**, 616–619 (2014).
27. Rasmussen, S. O. et al. A stratigraphic framework for abrupt climatic changes during the Last Glacial period based on three synchronized Greenland ice-core records: refining and extending the INTIMATE event stratigraphy. *Quat. Sci. Rev.* **106**, 14–28 (2014).
28. Su, Z., Ingersoll, A. P. & He, F. On the abruptness of Bölling-Allerød warming. *J. Clim.* **29**, 4965–4975 (2016).
29. Bard, E., Hamelin, B. & Delanghe-Sabatier, D. Deglacial meltwater pulse 1B and younger dryas sea levels revisited with boreholes at tahiti. *Science* **327**, 1235–1237 (2010).
30. Wagner, J. D. M. et al. Moisture variability in the southwestern United States linked to abrupt glacial climate change. *Nat. Geosci.* **3**, 110–113 (2010).
31. Fletcher, W. J. et al. Millennial-scale variability during the last glacial in vegetation records from Europe. *Quat. Sci. Rev.* **29**, 2839–2864 (2010).
32. Birks, H. H. South to north: contrasting late-glacial and early-Holocene climate changes and vegetation responses between south and north Norway. *Holocene* **25**, 37–52 (2015).
33. Giesecke, T., Brewer, S., Finsinger, W., Leydet, M. & Bradshaw, R. H. W. Patterns and dynamics of European vegetation change over the last 15,000 years. *J. Biogeogr.* **44**, 1441–1456 (2017).
34. Novello, V. F. et al. A high-resolution history of the South American Monsoon from Last Glacial Maximum to the Holocene. *Sci. Rep.* **7**, 44267 (2017).
35. Jaccard, S. L. & Galbraith, E. D. Large climate-driven changes of oceanic oxygen concentrations during the last deglaciation. *Nat. Geosci.* **5**, 151–156 (2012).
36. Reichert, G. J., Lourens, L. J. & Zachariasse, W. J. Temporal variability in the northern Arabian Sea oxygen minimum zone (OMZ) during the last 225,000 years. *Paleoceanography* **13**, 607–621 (1998).
37. Praetorius, S. K. et al. North Pacific deglacial hypoxic events linked to abrupt ocean warming. *Nature* **527**, 362–366 (2015).
38. Davies, M. H. et al. The deglacial transition on the southeastern Alaska Margin: meltwater input, sea level rise, marine productivity, and sedimentary anoxia. *Paleoceanography* **26**, PA2223 (2011).
39. Abdul, N. A., Mortlock, R. A., Wright, J. D. & Fairbanks, R. G. Younger Dryas sea level and meltwater pulse 1B recorded in Barbados reef crest coral *Acropora palmata*. *Paleoceanography* **31**, 330–344 (2016).
40. Soulet, G. et al. Glacial hydrologic conditions in the Black Sea reconstructed using geochemical pore water profiles. *Earth Planet. Sci. Lett.* **296**, 57–66 (2010).
41. Yanchilina, A. G. et al. Compilation of geophysical, geochronological, and geochemical evidence indicates a rapid Mediterranean-derived submergence of the Black Sea's shelf and subsequent substantial salinification in the early Holocene. *Mar. Geol.* **383**, 14–34 (2017).
42. Toucanne, S. et al. The first estimation of Fleuve Manche palaeoriver discharge during the last deglaciation: evidence for Fennoscandian ice sheet meltwater flow in the English Channel ca 20–18 ka ago. *Earth Planet. Sci. Lett.* **290**, 459–473 (2010).
43. Hanebuth, T., Statterger, K. & Grootes, P. M. Rapid flooding of the Sunda Shelf: a late-glacial sea-level record. *Science* **288**, 1033–1035 (2000).
44. Andersen, K. K. et al. High-resolution record of Northern Hemisphere climate extending into the last interglacial period. *Nature* **431**, 147–151 (2004).
45. Steffen, W. et al. Trajectories of the Earth system in the Anthropocene. *Proc. Natl Acad. Sci. USA* **115**, 8252–8259 (2018).
46. Buckley, B. M. et al. Climate as a contributing factor in the demise of Angkor, Cambodia. *Proc. Natl Acad. Sci. USA* **107**, 6748–6752 (2010).
47. Shuman, B. N. & Marsicek, J. The structure of Holocene climate change in mid-latitude North America. *Quat. Sci. Rev.* **141**, 38–51 (2016).
48. Alley, R. B. & Agustsdottir, A. M. The 8k event: cause and consequences of a major Holocene abrupt climate change. *Quat. Sci. Rev.* **24**, 1123–1149 (2005).
49. Tinner, W. & Lotter, A. F. Central European vegetation response to abrupt climate change at 8.2 ka. *Geology* **29**, 551–554 (2001).
50. Ellis, E. C. Anthropogenic transformation of the terrestrial biosphere. *Philos. Trans. R. Soc. A* **369**, 1010–1035 (2011).
51. Wang, Y. J. et al. A high-resolution absolute-dated Late Pleistocene monsoon record from Hulu Cave, China. *Science* **294**, 2345–2348 (2001).
52. Williams, J. W. & Burke, K. In *Climate Change and Biodiversity* (eds Lovejoy, T. & Hannah, L.) 128–141 (Yale Univ. Press, 2019).
53. deMenocal, P. et al. Abrupt onset and termination of the African Humid Period: rapid climate responses to gradual insolation forcing. *Quat. Sci. Rev.* **19**, 347–361 (2000).
54. Gupta, A., Das, M. & Anderson, D. Solar influence on the Indian summer monsoon during the Holocene. *Geophys. Res. Lett.* **32**, L17703 (2005).
55. Buntgen, U. et al. Cooling and societal change during the Late Antique Little Ice Age from 536 to around 660 AD. *Nat. Geosci.* **9**, 231–236 (2016).
56. Walker, M. et al. Formal subdivision of the holocene series/epoch: a summary. *J. Geol. Soc. India* **93**, 135–141 (2019).
57. Bradley, R. & Bakke, J. Is there evidence for a 4.6ka BP event in the northern North Atlantic region? *Clim. Past* **15**, 1665–1676 (2019).
58. Butzer, K. W. Collapse, environment, and society. *Proc. Natl Acad. Sci. USA* **109**, 3632–3639 (2012).
59. Shanahan, T. M. et al. The time-transgressive termination of the African Humid Period. *Nat. Geosci.* **8**, 140–144 (2015).
60. Trauth, M. H. et al. Classifying past climate change in the Chew Bahir basin, southern Ethiopia, using recurrence quantification analysis. *Clim. Dynam.* **53**, 2557–2572 (2019).
61. Claussen, M., Bathiany, S., Brovkin, V. & Kleinen, T. Simulated climate-vegetation interaction in semi-arid regions affected by plant diversity. *Nat. Geosci.* **6**, 954–958 (2013).
62. Kropelin, S. et al. Climate-driven ecosystem succession in the Sahara: the past 6000 years. *Science* **320**, 765–768 (2008).
63. Yeakel, J. D. et al. Collapse of an ecological network in Ancient Egypt. *Proc. Natl Acad. Sci. USA* **111**, 14472–14477 (2014).
64. Kuper, R. & Kropelin, S. Climate-controlled Holocene occupation in the Sahara: motor of Africa's evolution. *Science* **313**, 803–807 (2006).
65. Miao, X. D. et al. A 10,000 year record of dune activity, dust storms, and severe drought in the central Great Plains. *Geology* **35**, 119–122 (2007).
66. Williams, J. W., Shuman, B. & Bartlein, P. J. Rapid responses of the prairie-forest ecotone to early Holocene aridity in mid-continental North America. *Glob. Planet. Change* **66**, 195–207 (2009).
67. Williams, J. W., Blois, J. L. & Shuman, B. N. Extrinsic and intrinsic forcing of abrupt ecological change: case studies from the late Quaternary. *J. Ecol.* **99**, 664–677 (2011).
68. Umbanhowar, C. E., Camill, P., Geiss, C. E. & Teed, R. Asymmetric vegetation responses to mid-Holocene aridity at the prairie-forest ecotone in south-central Minnesota. *Quat. Res.* **66**, 53–66 (2006).
69. Williams, J. W., Shuman, B., Bartlein, P. J., Diffenbaugh, N. S. & Webb, T. Rapid, time-transgressive, and variable responses to early Holocene midcontinental drying in North America. *Geology* **38**, 135–138 (2010).
70. Shuman, B. Patterns, processes, and impacts of abrupt climate change in a warm world: the past 11,700 years. *WIREs Clim. Change* **3**, 19–43 (2012).
71. Bocinsky, R. K., Rush, J., Kintigh, K. W. & Kohler, T. A. Exploration and exploitation in the macrohistory of the pre-Hispanic Pueblo Southwest. *Sci. Adv.* **2**, e1501532 (2016).
72. Graybill, D. A., Gregory, D. A., Funkhouser, G. S. & Nials, F. In *Environmental Change and Human Adaptation in the Ancient American Southwest* (eds Doyel, D. E. & Dean, J. S.) 69–123 (Univ. Utah Press, 2006).
73. Scheffer, M. et al. Early-warning signals for critical transitions. *Nature* **461**, 53–59 (2009).
74. Dakos, V. et al. Slowing down as an early warning signal for abrupt climate change. *Proc. Natl Acad. Sci. USA* **105**, 14308–14312 (2008).
75. Wagner, T. J. W. & Eisenman, I. False alarms: how early warning signals falsely predict abrupt sea ice loss. *Geophys. Res. Lett.* **42**, 10333–10341 (2015).
76. Boulton, C. A., Good, P. & Lenton, T. M. Early warning signals of simulated Amazon rainforest dieback. *Theor. Ecol.* **6**, 373–384 (2013).
77. Held, H. & Kleinen, T. Detection of climate system bifurcations by degenerate fingerprinting. *Geophys. Res. Lett.* **31**, L23207 (2004).

78. Boulton, C. A., Allison, L. C. & Lenton, T. M. Early warning signals of atlantic meridional overturning circulation collapse in a fully coupled climate model. *Nat. Commun.* **5**, 5752 (2014).
79. Ditlevsen, P. D. & Johnsen, S. J. Tipping points: early warning and wishful thinking. *Geophys. Res. Lett.* **37**, L19703 (2010).
80. Cimadoribus, A. A., Drijfhout, S. S., Livina, V. & van der Schrier, G. Dansgaard-Oeschger events: bifurcation points in the climate system. *Clim. Past* **9**, 323–333 (2013).
81. Thomas, Z. A. et al. Early warnings and missed alarms for abrupt monsoon transitions. *Clim. Past* **11**, 1621–1633 (2015).
82. Stegner, M. A., Ratajczak, Z., Carpenter, S. R. & Williams, J. W. Inferring critical transitions in paleoecological time series with irregular sampling and variable time-averaging. *Quat. Sci. Rev.* **207**, 49–63 (2019).
83. Litzow, M. A., Urban, J. D. & Laurel, B. J. Increased spatial variance accompanies reorganization of two continental shelf ecosystems. *Ecol. Appl.* **18**, 1331–1337 (2008).
84. Bathiany, S., Claussen, M. & Fraedrich, K. Detecting hotspots of atmosphere-vegetation interaction via slowing down. Part 1: a stochastic approach. *Earth Syst. Dynam.* **4**, 63–78 (2013).
85. Weinans, E. et al. Finding the direction of lowest resilience in multivariate complex systems. *J. R. Soc. Interface* **16**, 20190629 (2019).
86. Feng, Q. Y., Viebahn, J. P. & Dijkstra, H. A. Deep ocean early warning signals of an Atlantic MOC collapse. *Geophys. Res. Lett.* **41**, 6009–6015 (2014).
87. Praetorius, S. K. & Mix, A. C. Synchronization of North Pacific and Greenland climates preceded abrupt deglacial warming. *Science* **345**, 444–448 (2014).
88. Guttal, V. & Jayaprakash, C. Spatial variance and spatial skewness: leading indicators of regime shifts in spatial ecological systems. *Theor. Ecol.* **2**, 3–12 (2009).
89. Rietkerk, M., Dekker, S. C., de Ruiter, P. C. & van de Koppel, J. Self-organized patchiness and catastrophic shifts in ecosystems. *Science* **305**, 1926–1929 (2004).
90. Dekker, M. M., von der Heydt, A. S. & Dijkstra, H. A. Cascading transitions in the climate system. *Earth Syst. Dynam.* **9**, 1243–1260 (2018).
91. Downey, S. S., Haas, W. R. & Shennan, S. J. European Neolithic societies showed early warning signals of population collapse. *Proc. Natl Acad. Sci. USA* **113**, 9751–9756 (2016).
92. Spielmann, K. A., Peeples, M. A., Glowacki, D. M. & Dugmore, A. Early warning signals of social transformation: a case study from the US Southwest. *PLoS ONE* **11**, e0163685 (2016).
93. Hsieh, C. H. et al. Fishing elevates variability in the abundance of exploited species. *Nature* **443**, 859–862 (2006).
94. Cailleret, M. et al. Early-warning signals of individual tree mortality based on annual radial growth. *Front. Plant Sci.* **9**, 1964 (2019).
95. Drake, J. M. & Griffen, B. D. Early warning signals of extinction in deteriorating environments. *Nature* **467**, 456–459 (2010).
96. Klose, A. K., Karle, V., Winkelmann, R. & Donges, J. F. Emergence of cascading dynamics in interacting tipping elements of ecology and climate. *R. Soc. Open Sci.* **7**, 200599 (2020).
97. Bathiany, S., Hidding, J. & Scheffer, M. Edge detection reveals abrupt and extreme climate events. *J. Clim.* **33**, 6399–6421 (2020).
98. Flach, M. et al. Multivariate anomaly detection for Earth observations: a comparison of algorithms and feature extraction techniques. *Earth Syst. Dynam.* **8**, 677–696 (2017).
99. Reeves, J., Chen, J., Wang, X. L. L., Lund, R. & Lu, Q. Q. A review and comparison of changepoint detection techniques for climate data. *J. Appl. Meteorol. Climatol.* **46**, 900–915 (2007).
100. Flato, G. M. Earth system models: an overview. *WIREs Clim. Change* **2**, 783–800 (2011).
101. Drijfhout, S. et al. Catalogue of abrupt shifts in Intergovernmental Panel on Climate Change climate models. *Proc. Natl Acad. Sci. USA* **112**, E5777–E5786 (2015).
102. Dallmeyer, A., Claussen, M., Lorenz, S. J. & Shanahan, T. The end of the African humid period as seen by a transient comprehensive Earth system model simulation of the last 8000 years. *Clim. Past* **16**, 117–140 (2020).
103. Turetsky, M. R. et al. Carbon release through abrupt permafrost thaw. *Nat. Geosci.* **13**, 138–143 (2020).

## Acknowledgements

This paper is an outcome of the workshop 'Abrupt changes, thresholds, and tipping points in Earth history and future implications' held in Hamburg, Germany, in November 2018, which most of the authors attended. The workshop was officially endorsed by Analysis, Integration and Modeling of the Earth System (AIMES) and Past Global Changes (PAGES) of Future Earth and received financial support from PAGES and the Max Planck Society. We thank N. Noreiks for assistance with Fig. 3. F.L. acknowledges funding from ANID/MSI/Millennium Nucleus Paleoclimate under grant number ANID/FONDAP/15110009 and grant number ANID/FONDECYT/1191223. J.M. was supported in part by the US NSF. J.W.W. acknowledges funding from NSF grant number 1855781 and WARE. V.B., T.K. and M. Claussen acknowledge support from the German Federal Ministry of Education and Research (BMBF) through the PalMod project. J.F.D. was supported by the Leibniz Association project DominoES and the European Research Council Advanced Grant project ERA (Earth Resilience in the Anthropocene; grant ERC-2016-ADG-743080).

## Author contributions

All authors contributed to the literature assessment. V.B., S.B., J.W.W., E.B. and T.M.L. developed the concept and compiled the paper with support from all co-authors. All co-authors contributed to the discussion of the manuscript.

## Competing interests

The authors declare no competing interests.

## Additional information

**Supplementary information** The online version contains supplementary material available at <https://doi.org/10.1038/s41561-021-00790-5>.

**Correspondence** should be addressed to V.B.

**Peer review information** *Nature Geoscience* thanks Cathy Whitlock and the other, anonymous, reviewer(s) for their contribution to the peer review of this work. Primary Handling Editor: James Super.

**Reprints and permissions information** is available at [www.nature.com/reprints](http://www.nature.com/reprints).

**Publisher's note** Springer Nature remains neutral with regard to jurisdictional claims in published maps and institutional affiliations.

© Springer Nature Limited 2021

**Supplementary information**

---

**Past abrupt changes, tipping points and cascading impacts in the Earth system**

---

In the format provided by the authors and unedited

## Annex 1. Calculation of abruptness rates

Our approach to calculate abruptness of changes during abrupt event follows the recent method<sup>1</sup>: we compare the rate of changes before the event and during the event. We calculate a ratio of these rates for the variable under consideration, such as atmospheric CO<sub>2</sub> concentration, and compare it with the ratio for the orbital forcing. The procedure is as follows. We define the abrupt event period  $T_{ab}$ ,  $t_1$  to  $t_2$ , and calculate rate of changes in variable under consideration,  $V(t)$ , during abrupt period. Because of interannual variability in  $V(t)$ , we use an average of variable of up to 200 years before and after the change to calculate the rate

$$R_{ab} = (\bar{V}(t_2) - \bar{V}(t_1)) / (t_2 - t_1) \quad (A1)$$

For the reference period,  $T_{ref}$ ,  $t_0$  to  $t_1$ , which is taken much longer than the period of abrupt changes, the rate of  $V$  changes,  $R_{ref}$ , is calculated as a slope of linear interpolation using Python package *lmfit*. The abruptness of changes relative to the reference period,  $A_{ab}$ , is calculated as a ratio  $R_{ab} / R_{ref}$ . The higher the value of  $A_{ab}$ , the more abrupt are changes relative to the reference period. Let us note that abruptness  $A_{ab}$  calculated in this way is not limited to time scale of changes, e.g. decadal or centennial, but is defined relative to the changes during the reference period.

To compare with the abruptness of the orbital forcing  $F(t)$ , we do the same procedure with the orbital forcing as above using a computational algorithm of long-term variations of insolation<sup>2</sup>. We use the same reference and abrupt change periods  $T_{ref}$  and  $T_{ab}$ , respectively. Because interannual variability in orbital forcing is negligible, we skip averaging of forcing before and after change and calculate the rate of changes in orbital forcing during the abrupt change period,  $O_{ab}$ , as

$$O_{ab} = (F(t_2) - F(t_1)) / (t_2 - t_1) \quad (A2)$$

For the reference period,  $T_{ref}$ ,  $t_0$  to  $t_1$ , the rate of orbital forcing changes,  $O_{ref}$ , is calculated as a slope of linear interpolation using Python package *lmfit*. The abruptness of changes relative to the reference period,  $A_{orb}$ , is calculated as a ratio  $O_{ab} / O_{ref}$ .

Finally, we calculate abruptness of changes in the variable relative to changes in the orbital forcing,  $A$ , as a ratio  $A_{ab} / A_{orb}$ . The values of intermediate variables and final rates are provided in Table A1 and illustrated in the Figure A1. To explain the procedure, let us follow an example of the Case 1 in the Table A1. The variable is atmospheric CO<sub>2</sub> concentration from the West Antarctic ice core<sup>3</sup>. The steps of calculating abruptness  $A$  are as follows:

- Firstly, from the CO<sub>2</sub> record, we visually defined an abrupt change period, 14.8 to 14.6 ka BP. Calculating average values in CO<sub>2</sub> during 200 years before the abrupt change, i.e. during 15.0 to 14.8 ka BP, and after the change, i.e. 14.6 to 14.4 kyr BP, we find an increase of 11.1 ppm during the abrupt change period. The rate of change  $R_{ab}$  is therefore 11.1 ppm/0.2 kyr, or 56 ppm kyr<sup>-1</sup>. The average concentrations before and after the change are shown as black horizontal lines in Fig. 1 (left), while the black line connecting them indicate a slope of change.

- Secondly, we linearly interpolate CO<sub>2</sub> concentrations during the reference period which we define as 16.0 to 14.8 ka BP. The rate of increase during the reference period,  $R_{ref}$ , is 5.9 ppm kyr<sup>-1</sup>, while a total change during the reference period is 7.1 ppm. The interpolation is shown as a blue line on Fig. 1, left. Consequently,  $A_{ab} = R_{ab} / R_{ref} = 56 \text{ ppm kyr}^{-1} / 5.9 \text{ ppm kyr}^{-1} = 9.5$ . For the orbital forcing, we assume that the relevant characteristic is an incoming solar radiation averaged over July at 65°N. Results of calculated changes during the abrupt change period and reference period are shown on Fig. 1 (right). The abruptness of orbital forcing,  $A_{orb}$ , is calculated as 1.08.
- Finally, an abruptness of changes in CO<sub>2</sub> concentration relative to the changes in orbital forcing,  $A$ , is  $A_{ab} / A_{orb} = 9.5 / 1.08$ , or 8.8.

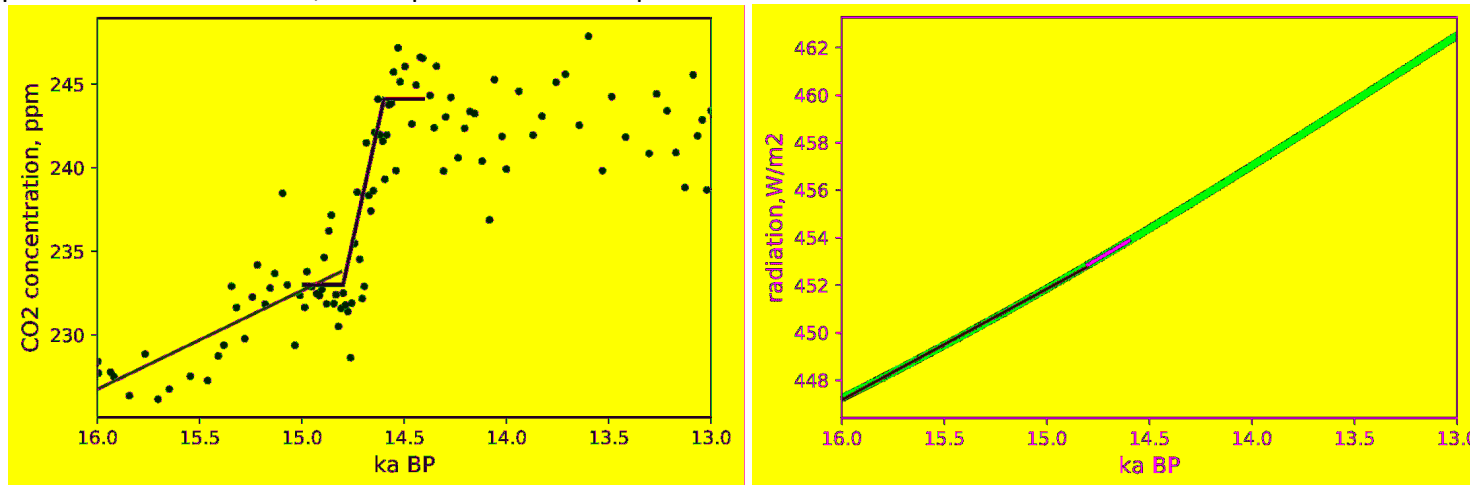
The abruptness of orbital forcing,  $A_{orb}$  is small (0.96-1.32), unless the reference period insolation change is small as for the case 7 of tree cover change in the Steel Lake record (2.45). Comparison of  $A_{ab}$  and  $A_{orb}$  shows that the change during the selected abrupt period is always substantially faster (3.4 to 89 times) than the change in orbital forcing. The abruptness  $A$  values in the Table A1 are in the range from 8 to 98, which we consider as significantly abrupt.

Table A1. Abruptness of changes for records shown in the Figure 3.

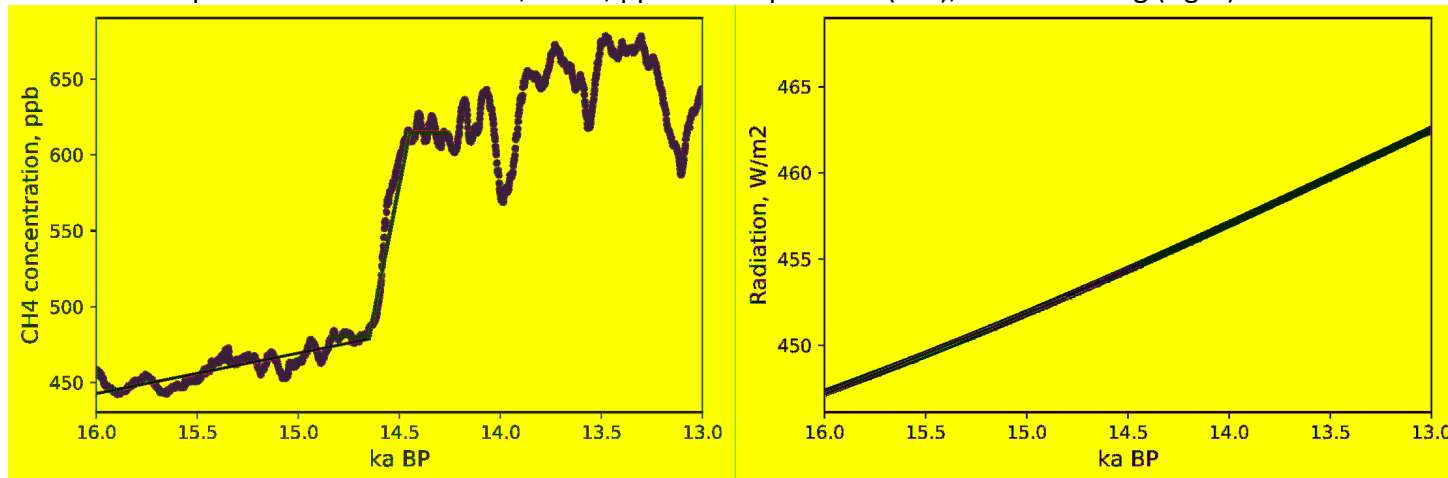
- The column “abrupt change period” shows: (i) the period with most abrupt changes,  $T_{ab}$ ; (ii) the amplitude of changes during this period calculated as a difference between averages of periods before-and after change (shown as horizontal black lines on the Fig. A1); (iii) the rate of changes during abrupt period,  $R_{ab}$ ;
- The column “reference period” shows characteristics as above, but for the reference period  $T_{ref}$ , including rates of changes  $R_{ref}$ ;
- “Abruptness relative to the reference period”,  $A_{ab}$  is calculated as a ratio  $R_{ab}/R_{ref}$ ;
- “Abruptness of orbital forcing (latitude)”:  $A_{ref}$ , the ratio of rate of changes in the orbital forcing during the abrupt change period (black lines on Fig. A1 plots) to the rate of change in orbital forcing during the reference period (blue lines). In parentheses, a latitude used in calculation of the orbital forcing.
- “Abruptness relative to the orbital forcing”:  $A$ , or ratio  $A_{ab}/A_{ref}$ .

Case Nr.	Variable	Abrupt change period, amplitude of changes, rate of changes	Reference period, amplitude of changes, rate of changes	Abruptness relative to the reference period	Abruptness of orbital forcing (latitude)	Abruptness relative to the orbital forcing
1	Atmospheric CO <sub>2</sub> concentration, WAIS, ppm <sup>3</sup>	14.8 to 14.6 ka BP, 11.1 ppm, 56 ppm kyr <sup>-1</sup>	16.0 to 14.8 ka BP, 7.1 ppm, 5.9 ppm kyr <sup>-1</sup>	9.5	1.08 (65°N)	8.8
2	Atmospheric CH <sub>4</sub> concentration, WAIS, ppb <sup>3</sup>	14.65 to 14.45 ka BP, 134 ppb, 672 ppb kyr <sup>-1</sup>	16.0 to 14.65 ka BP, 36 ppb, 27 ppb kyr <sup>-1</sup>	25	1.09 (65°N)	23
3	AMOC strength, <sup>231</sup> Pa/ <sup>230</sup> Th ratio, ppt <sup>4</sup>	14.65 to 14.45 ka BP, 22 ppt, 107 ppt kyr <sup>-1</sup>	16.0 to 14.65 ka BP, 1.5 ppt, 1.1 ppt kyr <sup>-1</sup>	98	1.09 (65°N)	89
4	N. Pacific hypoxia, <i>Bulimina exilis</i> , % <sup>5</sup>	14.9 to 14.7 ka BP, 43%, 216% kyr <sup>-1</sup>	16.0 to 14.9 ka BP, 3.7%, 3.4% kyr <sup>-1</sup>	64	1.06 (55°N)	58
5	Sea level, Barbados, m <sup>6</sup>	14.4 to 13.6 ka BP, 23 m, 29 m kyr <sup>-1</sup>	18.2 to 14.4 ka BP, 14 m, 3.7 m kyr <sup>-1</sup>	7.8	1.35 (65°N)	5.8
6	Tree cover, Iberian margin, % <sup>7</sup>	15.0 to 14.5 ka BP, 27%, 54% kyr <sup>-1</sup>	17.0 to 15.0 ka BP, 11%, 5.3% kyr <sup>-1</sup>	10	1.1 (35°N)	9
7	Tree cover, Steel Lake, % <sup>8</sup>	8.3 to 7.9 ka BP, -41%, -103% kyr <sup>-1</sup>	9.0 to 8.3 ka BP, -8.4%, -12% kyr <sup>-1</sup>	8.6	2.45 (45°N)	3.4
8	Drought index, Chew Bahir basin, Africa <sup>9</sup>	7.9 to 7.7 ka BP, 1.11, 5.6 kyr <sup>-1</sup>	9.0 to 7.9 ka BP, 0.41, 0.37 kyr <sup>-1</sup>	15	1.32 (5°N)	11
9	Dust increase, ODP 658C, % <sup>10</sup>	5.6 to 5.3 ka BP, 13.5%, 45% kyr <sup>-1</sup>	7.0 to 5.6 ka BP, 2.7%, 1.9% kyr <sup>-1</sup>	24	1.10 (25°N)	22
10	Drought index (PDSI), Angkor <sup>11</sup>	0.63 to 0.6 ka BP, -3.6, -120 kyr <sup>-1</sup>	0.7 to 0.63 ka BP, -0.87, -12.4 kyr <sup>-1</sup>	9.7	0.96 (15°N)	10

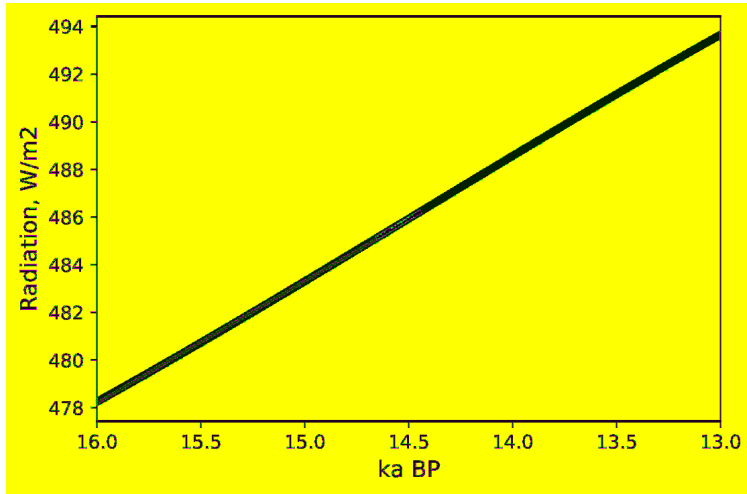
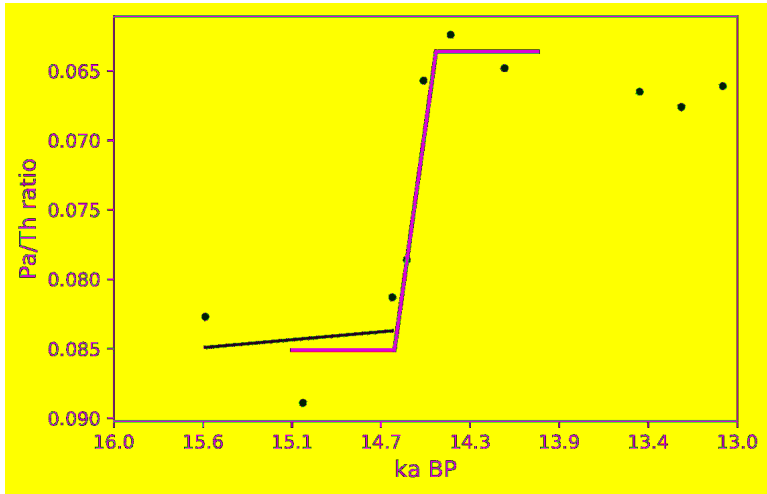
Figure A1. Graphical illustration of calculation of abruptness of changes in variables (left) and orbital forcing (right) for cases in Table A1. Red dots and lines are for variable and orbital forcing values, respectively. Blue line, trend in the reference period; black line – in the abrupt change period. For more details, see explanation of abruptness calculation above.



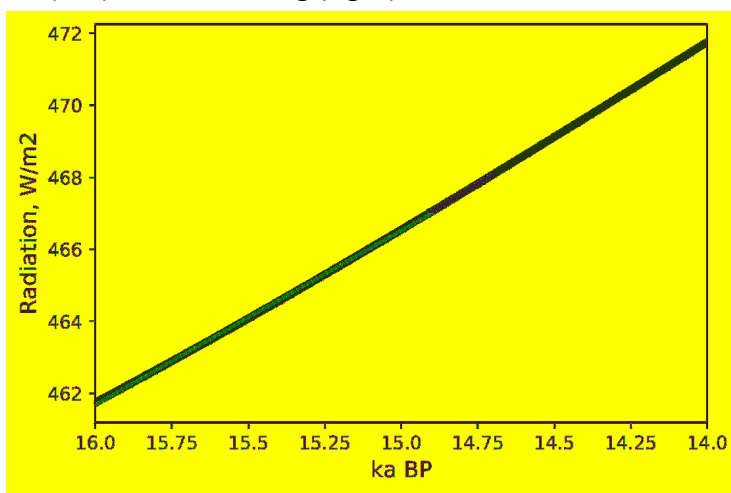
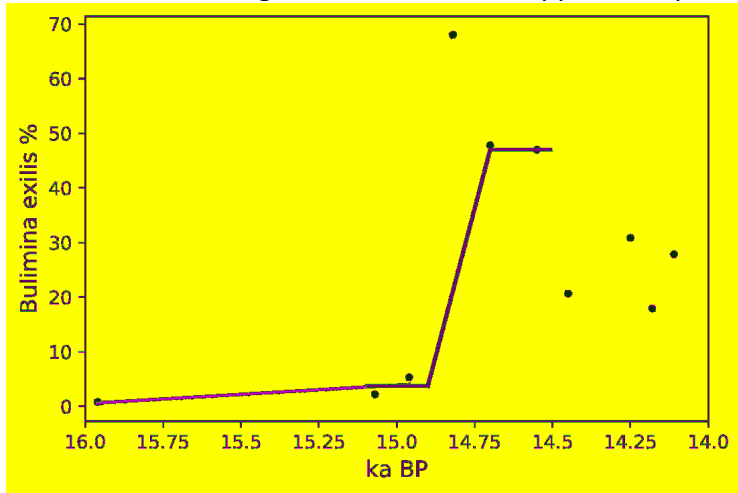
Case 1. Atmospheric CO<sub>2</sub> concentration, WAIS, ppm<sup>3</sup>. Abrupt series (left); orbital forcing (right).



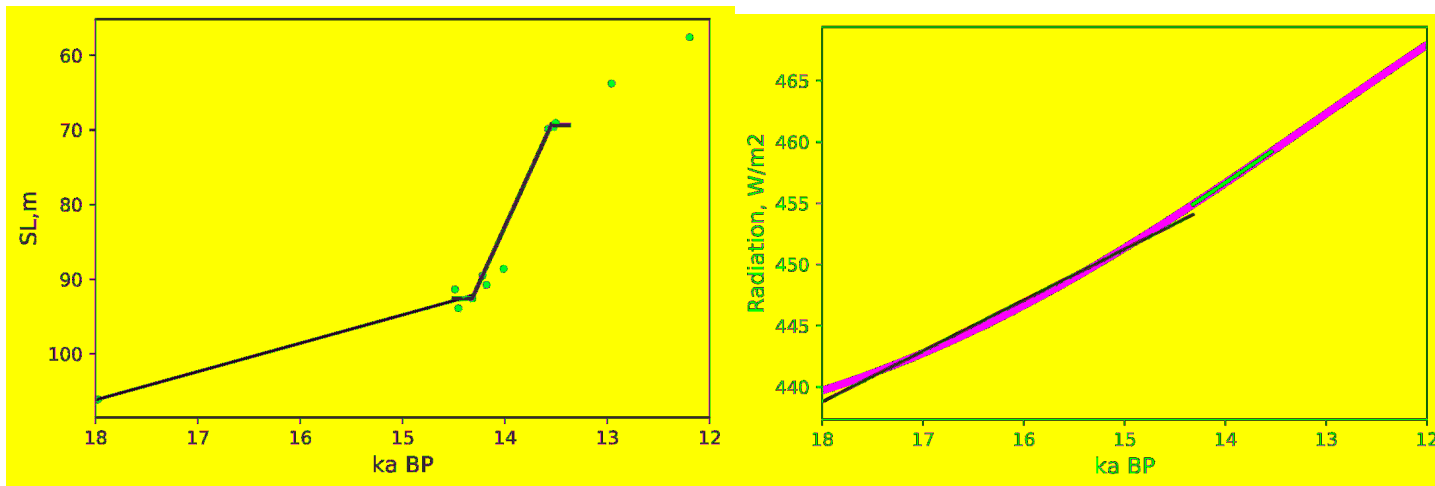
Case 2. Atmospheric CH<sub>4</sub> concentration, WAIS, ppb<sup>3</sup>. Abrupt series (left); orbital forcing (right)



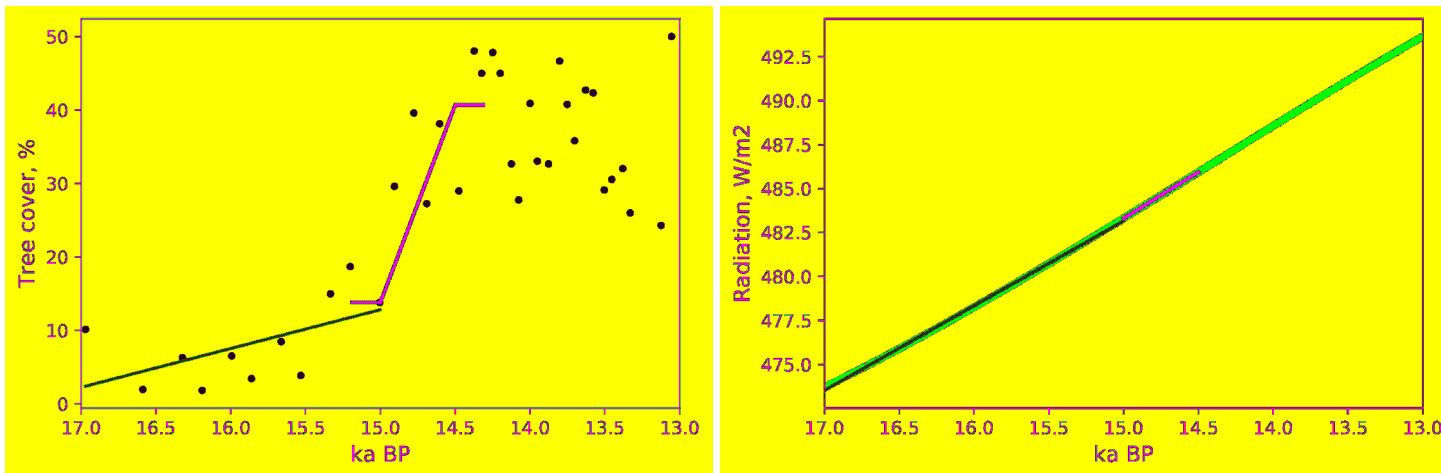
Case 3. AMOC strength,  $^{231}\text{Pa}/^{230}\text{Th}$  ratio, ppt<sup>4</sup>. Abrupt series (left); orbital forcing (right)



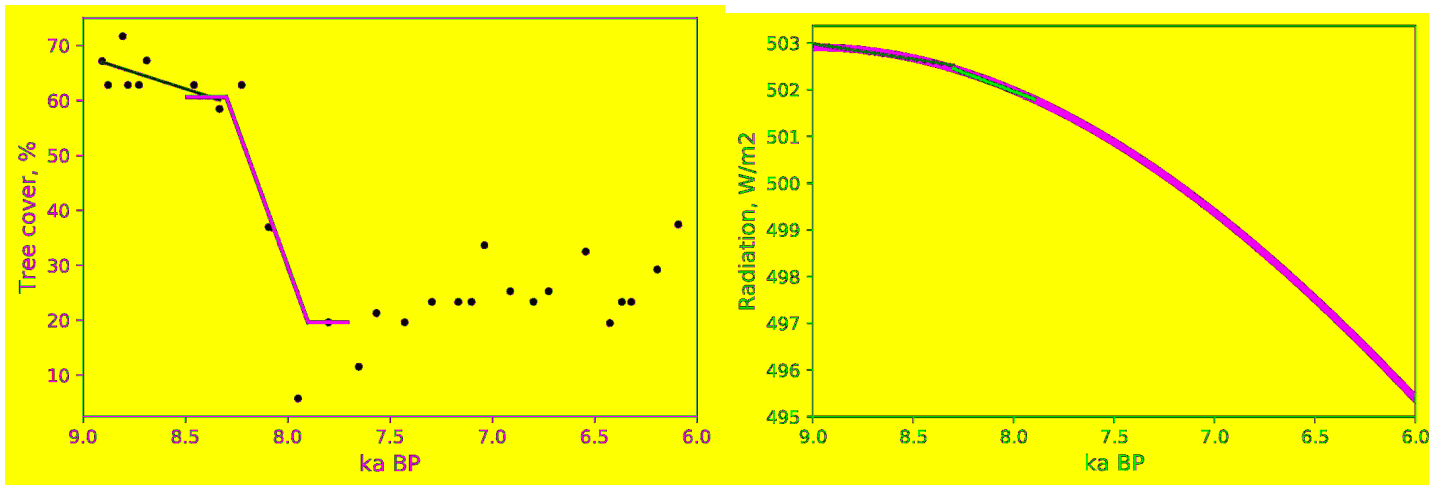
Case 4. N. Pacific hypoxia, *Bulimina exilis*, %<sup>5</sup>. Abrupt series (left); orbital forcing (right)



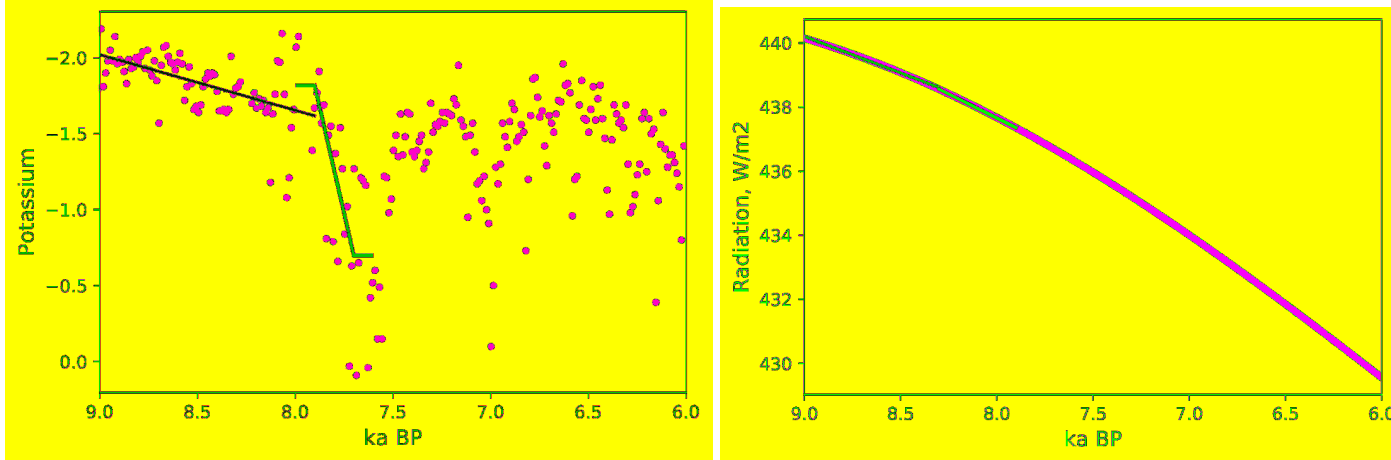
Case 5. Sea level, Barbados, m<sup>6</sup>. Abrupt series (left); orbital forcing (right)



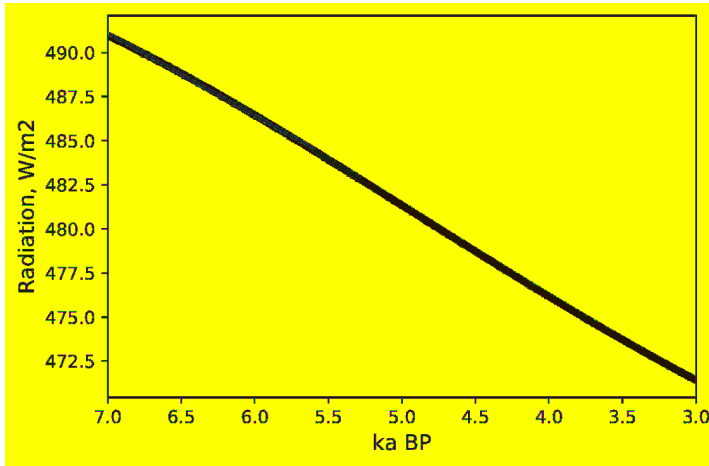
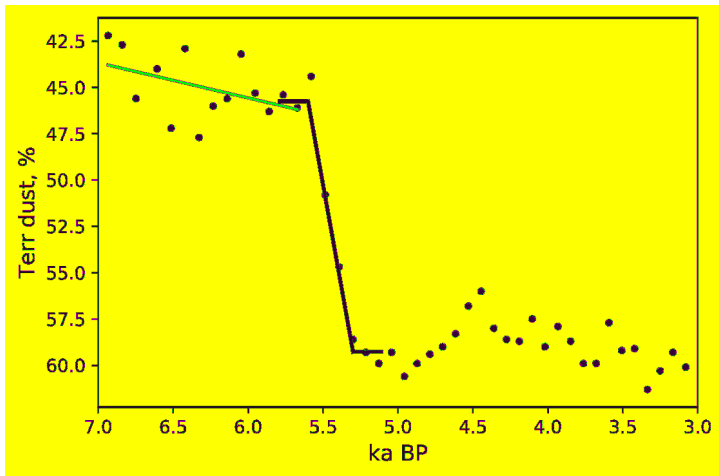
Case 6. Tree cover, Iberian margin, %<sup>7</sup>. Abrupt series (left); orbital forcing (right)



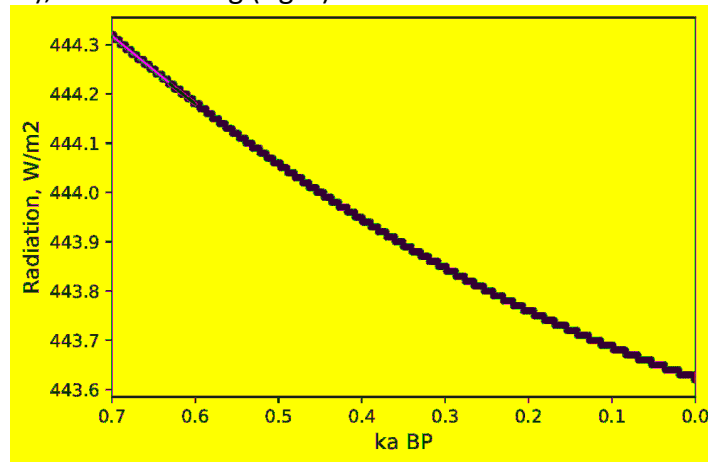
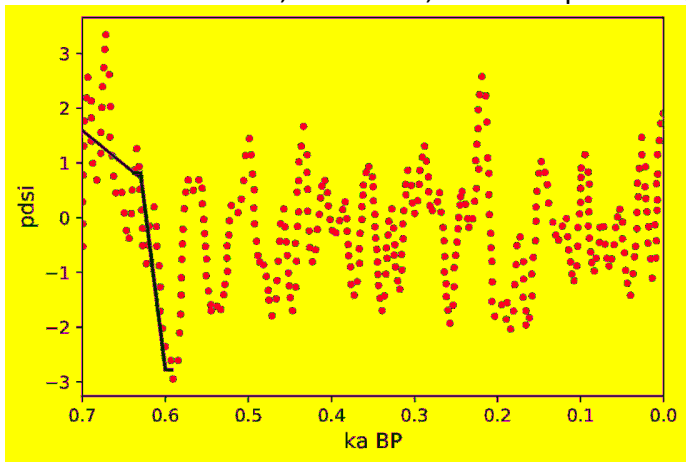
Case 7. Tree cover, Steel Lake, %<sup>8</sup>. Abrupt series (left); orbital forcing (right)



Case 8. Drought index, Chew Bahir basin, Africa<sup>9</sup>. Abrupt series (left); orbital forcing (right)



Case 9. Dust increase, ODP 658C, %<sup>10</sup>. Abrupt series (left); orbital forcing (right)



Case 10. Drought index (PDSI), Angkor<sup>11</sup>. Abrupt series (left); orbital forcing (right)

## References

- 1 Bathiany, S., Hidding, J. & Scheffer, M. Edge Detection Reveals Abrupt and Extreme Climate Events. *Journal of Climate* **33**, 6399–6421, doi:10.1175/JCLI-D-19-0449.1 (2020).
- 2 Berger, A. L. Long-term variations of daily insolation and quaternary climatic changes. *Journal of the Atmospheric Sciences* **35**, 2362-2367 (1978).
- 3 Marcott, S. A. *et al.* Centennial-scale changes in the global carbon cycle during the last deglaciation. *Nature* **514**, 616–+, doi:10.1038/nature13799 (2014).
- 4 McManus, J. F., Francois, R., Gherardi, J. M., Keigwin, L. D. & Brown-Leger, S. Collapse and rapid resumption of Atlantic meridional circulation linked to deglacial climate changes. *Nature* **428**, 834-837, doi:10.1038/nature02494 (2004).
- 5 Praetorius, S. K. *et al.* North Pacific deglacial hypoxic events linked to abrupt ocean warming. *Nature* **527**, 362–+, doi:10.1038/nature15753 (2015).
- 6 Abdul, N. A., Mortlock, R. A., Wright, J. D. & Fairbanks, R. G. Younger Dryas sea level and meltwater pulse 1B recorded in Barbados reef crest coral *Acropora palmata*. *Paleoceanography* **31**, 330-344, doi:10.1002/2015pa002847 (2016).
- 7 Goni, M. F. S. *et al.* Contrasting impacts of Dansgaars-Oeschger events over a western European latitudinal transect modulated by orbital parameters (vol 27, pg 1136, 2008). *Quaternary Science Reviews* **27**, 1789-1789, doi:10.1016/j.quascirev.2008.03.003 (2008).
- 8 Williams, J. W., Shuman, B., Bartlein, P. J., Diffenbaugh, N. S. & Webb, T. Rapid, time-transgressive, and variable responses to early Holocene midcontinental drying in North America. *Geology* **38**, 135-138, doi:10.1130/g30413.1 (2010).
- 9 Trauth, M. H. *et al.* Classifying past climate change in the Chew Bahir basin, southern Ethiopia, using recurrence quantification analysis. *Climate Dynamics* **53**, 2557-2572, doi:10.1007/s00382-019-04641-3 (2019).
- 10 deMenocal, P. *et al.* Abrupt onset and termination of the African Humid Period: rapid climate responses to gradual insolation forcing. *Quaternary Science Reviews* **19**, 347-361, doi:10.1016/s0277-3791(99)00081-5 (2000).
- 11 Buckley, B. M. *et al.* Climate as a contributing factor in the demise of Angkor, Cambodia. *Proceedings of the National Academy of Sciences of the United States of America* **107**, 6748-6752, doi:10.1073/pnas.0910827107 (2010).